A racetrack mode-locked silicon evanescent laser

Alexander W. Fang, Brian R. Koch, Kian-Giap Gan, Hyundai Park, Richard Jones, Oded Cohen, Mario J. Paniccia, Daniel J. Blumenthal, and John. E. Bowers

[1]*University of California, Santa Barbara, Department of Electrical and Computer Engineering, Santa Barbara, CA 93106, USA*
[2]*Intel Corporation, 2200 Mission College Blvd, SC12-326, Santa Clara, California 95054, USA*
[3]*Intel Corporation, S.B.I. Park Har Hotzvim, Jerusalem, 91031, Israel*
awfang@ece.ucsb.edu

Abstract: By utilizing a racetrack resonator topography, an on-chip mode locked silicon evanescent laser (ML-SEL) is realized that is independent of facet polishing. This enables integration with other devices on silicon and precise control of the ML-SEL's repetition rate through lithographic definition of the cavity length. Both passive and hybrid mode-locking have been achieved with transform limited, 7 ps pulses emitted at a repetition rate of 30 GHz. Jitter and locking range are measured under hybrid mode locking with a minimum absolute jitter and maximum locking range of 364 fs, and 50 MHz, respectively.

OCIS codes: (140.5960) Semiconductor lasers; (250.5300) Photonic integrated circuits.

References and links

1. G. T. Reed, "The optical age of silicon," Nature **427**, 615−618 (2004).
2. G. T. Reed and A. P. Knights, *Silicon Photonics: An Introduction* (John Wiley, Chichester, West Sussex, 2004).
3. L. Pavesi and D. J. Lockwood, *Silicon Photonics*, (Springer-Verlag, Berlin, 2004).
4. D. A. Miller, "Optical interconnects to silicon," IEEE J. Sel. Top Quantum. Electron. **6**, 1312−1317 (2000).
5. A. W. Fang, H. Park, O. Cohen, R. Jones, M. J. Paniccia, and J. E. Bowers, "Electrically pumped hybrid AlGaInAs-silicon evanescent laser," Opt. Express **14**, 9203-9210 (2006).
6. H. Park, A. W. Fang, R. Jones, O. Cohen, M. J. Paniccia, and J. E. Bowers, "40 C Continuous-Wave Electrically Pumped Hybrid Silicon Evanescent Laser," International Semiconductor Laser Conference 2006 (ISLC 2006), post deadline paper, September 2006.
7. B. R. Koch, A. W. Fang, O. Cohen, and J. E. Bowers, "Mode -locked silicon evanescent lasers," Opt. Express **15**, 11225-11233 (2007).
8. E. A. Avrutin, J. H. Marsh, and E. L. Portnoi, "Monolithic and multi-gigahertz mode locked semiconductor lasers: constructions, experiments, models, and applications," IEE Proc. Optoelectron. **147**, 251-278 (2000).
9. T. Ohno, H. Ishii, S. Matsuo, H. Okamoto, Y. Kawaguchi, Y, kondo, T. Furata, H. Ito, and Y. Yoshikuni, "Hybrid Modelocking of semiconductor ring lasers incorporating passive deep-ridge waveguides," Electron. Lett. **38**, 884-886 (2002).
10. Y. Barbarin, E. A. J. M. Bente, M. J. R. Heck, Y. S. Oei, R. Nötzel and M. K. Smit, "Characterization of a 15 GHz integrated bulk InGaAsP passively modelocked ring laser at 1.53μm," Opt. Express **14**, 9716 (2006).
11. S. Yu, T. F. Krauss, and P. J. R. Laybourn, "Mode Locking in large monolithic semiconductor ring lasers," Proc. SPIE **3278**, 139-148 (1998).
12. H. Boudinov, H. H. Tan, and C. Jagadish, "Electrical isolation n of n-type and p-type InP layers by proton bombardment," J. Appl. Phys. **89-10**, 5343-5347 (2001).
13. H. Park, A. W. Fang, R. Jones, O. Cohen, M. J. Paniccia, and J. E. Bowers, "A hybrid AlGaInAs-silicon evanescent waveguide photodetector," Opt. Express **15**, 6044-6052 (2007).

1. Introduction

The drive to utilize the low cost infrastructure of CMOS compatible foundry processes has resulted in an increased focus on silicon as a photonic integration platform [1-4]. A silicon evanescent device architecture that consists of crystalline III-V active regions transferred to silicon waveguides has been used to demonstrate electrically pumped lasers on silicon. This hybrid architecture overcomes the alignment and yield challenges of flip-chip laser bonding,

#90749 - $15.00 USD Received 11 Dec 2007; revised 15 Jan 2008; accepted 15 Jan 2008; published 17 Jan 2008

and allows for a high volume manufacturing process [5-6]. Recently, this platform was used to demonstrate mode locked silicon evanescent lasers (ML-SELs) with repetition rates of 40 GHz and 10 GHz [7]. These lasers utilize Fabry-Pérot topographies and rely on facet dicing and polishing to create mirrors. This leads to cavity length targeting errors on the order of ~30 microns altering the repetition rate by 1.2 GHz and 0.075 GHz at repetition rates of 40 GHz and 10 GHz, respectively. More importantly the use of facets makes these lasers impossible to integrate serially with other photonic devices on a single chip due to the discrete nature of the device. In this letter we present the first demonstration of a racetrack ML-SEL. The mode locked repetition rate is defined purely by lithographic fabrication processes, leading to precise frequency control and enabling integration into more complex photonic integrated circuits [8-11].

2. Device topography and experimental setup

The racetrack ML-SEL was fabricated utilizing the silicon evanescent device platform. The detailed fabrication process and epitaxial layer structure are described in [5]. The waveguide structure consists of an 8 AlGaInAs quantum well active layer structure bonded to a silicon rib waveguide with a waveguide width, height, and rib etch of 1.5 μm, 0.71 μm, and 0.49 μm, respectively. This results in confinement factors of 59.5% in silicon and 5.2% in the quantum wells as calculated with the film mode matching (FMM) method.

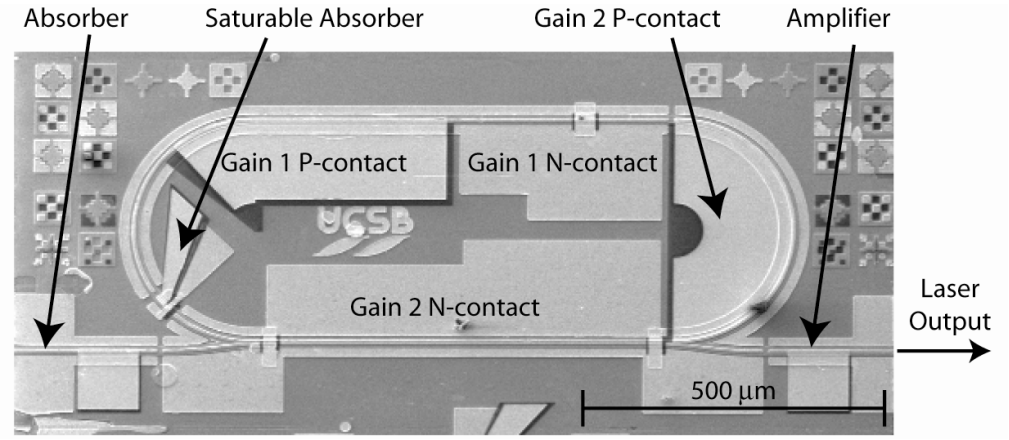

Fig. 1. Scanning electron micrograph of a racetrack mode locked silicon evanescent laser.

The device scanning electron micrograph image is shown in Fig. 1. The 2.657 mm long racetrack resonator consists of a 30 μm long saturable absorber and two gain sections with lengths of 1.13 mm and 1.467 mm. These sections are separated by 10 μm long unpumped regions that have undergone proton implantation to achieve electrical isolation [12]. The two gain sections 1 and 2 are both forward biased in parallel at 410 mA. The saturable absorber is DC biased with -0.66 volts under passive mode locking operation while an additional RF signal is applied to the saturable absorber under hybrid mode locking. Mode-locking occurs via colliding pulse mode-locking (CPM) with clockwise and counter clockwise pulses colliding simultaneously in the saturable absorber at a rate ~30 GHz as determined by the cavity length and group index of refraction. The output amplifier is biased at 47 mA producing an estimated ~4dB of gain based on the current density and length [13]. The device is temperature stabilized on a stage held at 10 °C.

Light is coupled out of the resonator through a 400 μm long directional coupler. The coupling ratio of the directional coupler is measured by launching light beyond the absorption range of the quantum wells through the bus waveguide of the directional coupler. The transmission spectra is collected at the other end of the bus where its finesse and extinction ratio are used to find the coupling ratio and cavity round trip loss. The coupling ratio was

#90749 - $15.00 USD Received 11 Dec 2007; revised 15 Jan 2008; accepted 15 Jan 2008; published 17 Jan 2008

measured at 1620 nm to be 55%. We estimated a coupling ratio of ~40% at 1590 nm by using Beamprop to simulate the modal dispersion of the coupler. The round trip loss was measured at 13 dB, which corresponds to a modal loss of 11 cm^{-1}. The coupler output facets were diced, polished, and anti-reflection coated with a single layer quarter wavelength Ta_2O_5 dielectric coating. The clockwise lasing pulses are coupled out of the resonator into a reverse biased section of active region acting as an anti-reflection absorber. The counter-clockwise lasing pulses are coupled out of the resonator and amplified through an integrated SOA before being collected by a lensed fiber. The coupling loss was measured to be 13 dB by reverse biasing the amplifier and measuring the detected photocurrent and comparing this to the fiber coupled output power. In order to avoid removal of critical device components, facet polishing was minimal, leading to poor facet quality and the resulting higher coupling losses than previously reported [5].

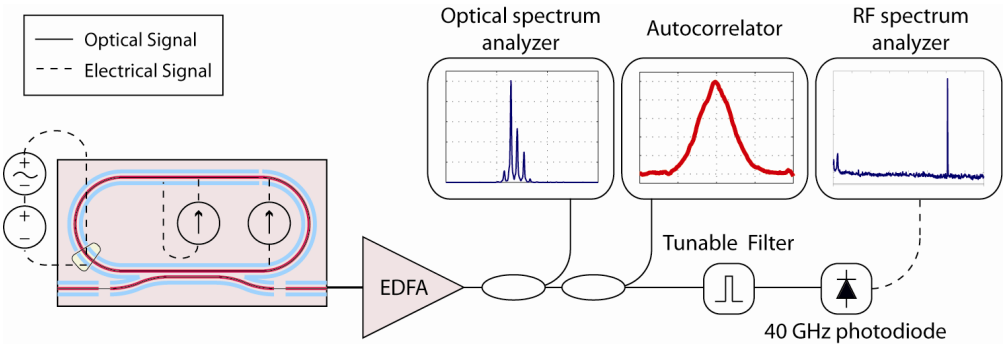

Fig. 2. Racetrack ML-SEL experimental set up.

The device characteristic measurement set up allows simultaneous monitoring of the pulse train in the wavelength domain, time domain, and RF frequency domain, as shown in Fig. 2. The ML-SEL pulses were collected by a lensed fiber and amplified through an EDFA. The signal is first split with 50% going to an optical spectrum analyzer, and the other 50% to a second 50/50 splitter. The outputs of the second splitter are sent to an autocorrelator and through a 1.2 nm wide tunable notch filter to a 40 GHz bandwidth photodetector. The electrical signal from the photodetector is sent to a DC - 41 GHz RF spectrum analyzer.

3. Experimental results

When all sections (gain 1, gain 2, and the saturable absorber) are connected and forward biased together in parallel, the laser threshold was measured to be 250 mA. The autocorrelator pulse traces for passive mode-locking and hybrid mode-locking are showed in Fig. 3(a). It can be seen that traces under these two modes of operation are almost identical. The auto-correlated pulse width was measured at 10 ps. A 7 ps pulse width is estimated by assuming a Gaussian pulse shape. The pulse width as a function of saturable absorber bias is shown in Fig. 4(b), with a minimum at the reported bias of -0.66V. The average power of the counter clockwise pulses is measured at 1.92 mW by reverse biasing the right SOA and measuring the collected photocurrent. We assume 100% internal quantum efficiency for the SOA acting as a photodetector to underestimate the power of the laser. This corresponds to a peak pulse power of 8.57 mW by taking into account the repetition rate of the laser and Gaussian pulse shape. The optical spectrum under passive and hybrid mode-locking is shown in Fig. 4. It can be seen that the spectrum does not change noticeably between these two mode-locking modes. The optical spectrum is centered at 1588.75 nm has a 0.5 nm spectral width. This corresponds to a time bandwidth product of 0.42, indicating that the pulses are transform limited.

#90749 - $15.00 USD Received 11 Dec 2007; revised 15 Jan 2008; accepted 15 Jan 2008; published 17 Jan 2008

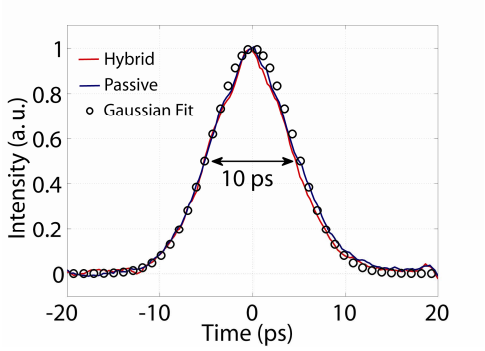

(a)

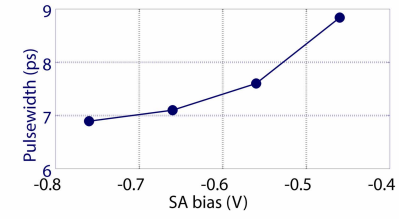

(b)

Fig. 3. (a). Passive mode-locked and hybrid mode-locked autocorrelation trace.(b) De-convolved pulse width versus saturable absorber bias.

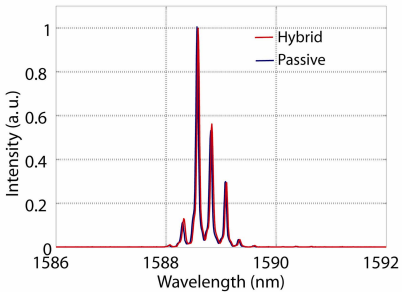

Fig. 4. The passive and hybrid mode-locked optical spectrum. The spectrum does not change noticeably between the two mode-locking modes.

The RF spectrum is shown in Fig. 5(a) under passive and hybrid mode locking with a 13 dBm 30.35 GHz RF signal. It can be seen that for hybrid mode locking, the RF spectrum narrows substantially, indicating a large reduction in signal jitter. Figure 5(b) shows the passively mode locked and actively mode locked RF spectrum over a range of 40 GHz. It can be seen that the extinction ratio between the 30 GHz tone and the device relaxation resonance is greater than 45 dB, giving clear evidence of mode locking. In addition, the 30 GHz tone is greater than 40 dB above the measurement noise floor. The absolute timing jitter was calculated by integrating two times the single sideband noise of the mode locking RF peak. Figure 6 shows the jitter under hybrid mode locking versus the upper integration limit. It can be seen that for the frequency range of 1 kHz to 100 MHz offset from the repetition frequency, the laser has an absolute jitter of 364 fs which is well below the ITU specification of 3.3ps for digital transmission at a 30 GHz repetition rate (0.1 times the bit period).

#90749 - $15.00 USD Received 11 Dec 2007; revised 15 Jan 2008; accepted 15 Jan 2008; published 17 Jan 2008

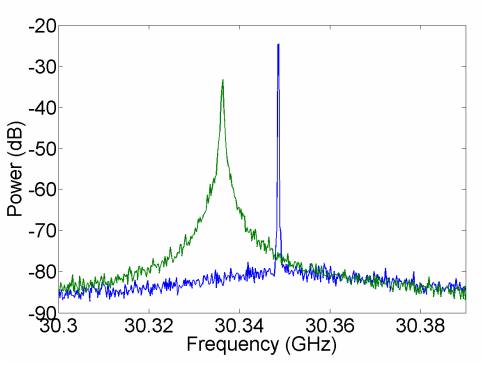

(a)

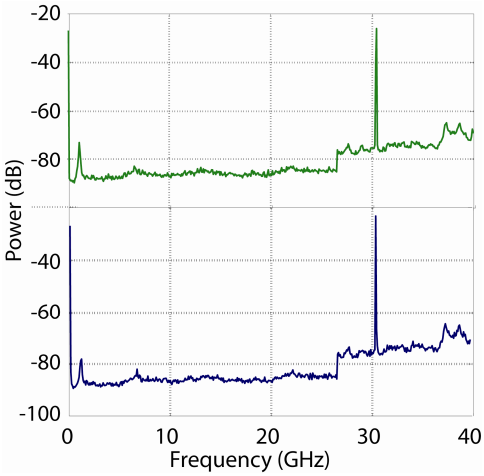

(b)

Fig. 5. (a). RF spectrum of passively and hybridly locked mode locked laser measured with a 10 kHz resolution bandwidth. (b). Wide RF spectrum of the MLL under passive locking (green) and hybrid locking (blue).

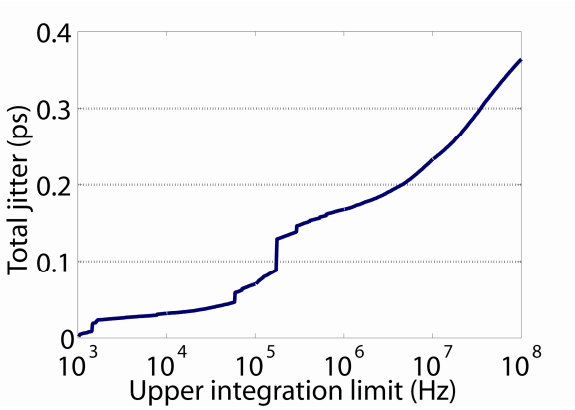

Fig. 6. Jitter shown for single side band integration ranges from 1 kHz to 100 MHz.

The dependence of the hybrid mode locked performance on drive power when driven with the fundamental (30 GHz) drive frequency is shown in Fig. 7. As expected, the jitter reduces

#90749 - $15.00 USD Received 11 Dec 2007; revised 15 Jan 2008; accepted 15 Jan 2008; published 17 Jan 2008

while the locking range increases with RF power with a maximum measured locking range of 50 MHz at 13.5 dBm. Since the cavity length is lithographically defined, only variations in the repetition rate detuning or group index of refraction can cause inconsistencies in the repetition rate among different devices. These inconsistencies could result from material variations, waveguide dimension variations, or other processing inconsistencies, but are likely to be very small for devices with the same design. The locking range of this device should easily compensate for any variation among different devices and fabrication process runs. It is likely that much lower locking ranges, such as those for low RF injection powers, would also be sufficient to achieve precise, repeatable mode locking frequencies using this type of device.

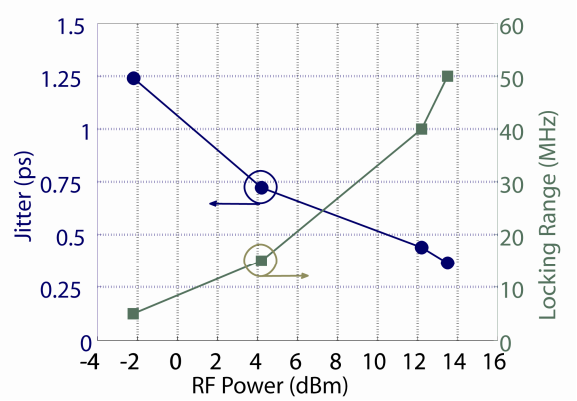

Fig. 7. Jitter measured with a 1 kHz-100 MHz integration range and locking range versus RF powers for fundamental and sub-harmonic synchronization.

4. Conclusion

An on-chip mode locked laser on silicon has been demonstrated with a repetition rate, and pulse width of 30 GHz, and 7 ps, respectively. Both passive and hybrid mode-locking have been achieved with the hybrid mode-locking showing a minimum jitter of 364 fs, making it well within the ITU specifications for digital data transmission. The repetition rate can easily be scaled beyond 30 GHz by modifying the cavity length. In addition, the silicon fabrication process in racetrack topographies only relies on a single rib waveguide etch process making it simple to precisely and repeatedly determine the mode locked frequency. The racetrack ring topography offers broad band feedback through its use of directional couplers as opposed to narrow band Bragg reflectors and can be engineered further to yield wide frequency combs for WDM source applications.

Acknowledgments

The authors would like to thank J. Mack, H. Poulsen, J. Shah, and W. Chang for insightful discussions and G. Zeng and H.-W. Chen, for help with device fabrication. This work was supported by a grant from Intel Corp. and from DARPA/MTO DODN program and ARL under award number W911NF-05-1-0175 and W911NF-04-9-0001.

#90749 - $15.00 USD Received 11 Dec 2007; revised 15 Jan 2008; accepted 15 Jan 2008; published 17 Jan 2008